Journal of Magnetic Resonance 205 (2010) 224–234

Contents lists available at ScienceDirect

Journal of Magnetic Resonance

journal homepage: www.elsevier.com/locate/jmr

Ultrafast T_1–T_2 relaxometry using FLOP sequences

Luca Venturi, Kevin Wright, Brian Hills *

Institute of Food Research, Norwich Research Park, Colney, Norwich NR4 7UA, UK

ARTICLE INFO

Article history:
Received 19 October 2009
Revised 29 April 2010
Available online 7 May 2010

Keywords:
FLOP
Longitudinal relaxation
Transverse relaxation
2D relaxometry

ABSTRACT

By periodically flipping the longitudinal magnetisation with a chain of 180° pulses it is possible to establish a steady-state of longitudinal polarisation that effectively stores the information of T_1 relaxation. The pulse sequence for achieving this, called steady-state Flipped LOngitudinal Polarisation (FLOP) can be used for the fast acquisition of a two-dimensional T_1–T_2 relaxation time spectrum in both periodic and a-periodic modes. We have therefore called this new class of sequences periodic or a-periodic FLOP–T_1–T_2.

1. Introduction

2D T_1–T_2 relaxation spectra based on the fast 2D inverse Laplace transformation algorithm developed by Song and Hurlimann [1,2] have proved invaluable as microstructural probes of a wide variety of complex, heterogeneous systems including porous rocks [1,3], cellular tissue [4,5], protein systems [6] and even nano-structured synthetic hydrogels [7]. There is also reason to believe that T_1–T_2 spectra could act as biomarkers in clinical diagnosis [8,9]. However the development of routine clinical T_1–T_2 relaxometry requires that it is both fast and volume-selective. A number of approaches to fast T_1–T_2 data acquisition have been proposed, including reducing the recovery delay [8] and multislicing [10]. We have also proposed a number of strategies for volume-selective T_1–T_2 relaxometry [11]. However steady-state methods based on the periodic inversion of longitudinal magnetisation have yet to be explored and have the potential of being faster than both the multislicing and reduced recovery delay methods.

Periodic inversion of the longitudinal magnetisation with a chain of 180° pulses eventually establishes a steady-state in the longitudinal magnetisation such that the magnetisation is periodically restored to some constant value. The CPMG sequence, that is routinely used to measure transverse relaxation, itself comprises a chain of equally spaced 180° pulses and will also establish a steady-state in the longitudinal magnetisation provided sufficient pulses (or spin-echoes) are used. In this paper we show how this fact can be used to output a discrete two-dimensional T_1–T_2 relaxation spectrum. We also show how the idea can be generalised into periodic and aperiodic pulse sequences and further sub-classified into those periodic sequences with separate or combined preparation and acquisition steps. The class of sequences based on repeated application of 180° inversion pulses can be called "FLOP" for "Flipped LOngitudinal Polarisation". Following this nomenclature, the present paper analyses the class of periodic and aperiodic FLOP–T_1–T_2 sequences. Elsewhere [12] we have reported that the FLOP methodology can be used for fast imaging with image contrast based on the degree of steady-state longitudinal magnetisation.

For clinical applications FLOP–T_1–T_2 methods need to be not only fast but also volume-selective where the volume selectivity needs to destroy longitudinal magnetisation outside the volume of interest (VOI) while preserving longitudinal and transverse magnetisation within the VOI. We have called the new sequence for achieving this the 'magic-SPACE box' because it can be inserted into a periodic FLOP sequence and is a simple variation of the well-known SPACE sequence [13].

This paper focuses mainly on the theoretical development of the FLOP–T_1–T_2 method, which is discussed at length in Section 2 and the experimental verification is performed only on simple doped water and oil phantoms in Section 4. The application to complex heterogeneous biological samples in clinical MRI scanners will be the subject of future work.

2. Periodic FLOP sequences

2.1. Theoretical analysis of periodic FLOP sequences with separate preparation and acquisition

Any periodically repeating pattern of 180° inversion pulses will eventually establish a "steady-state" in the longitudinal magnetisation whereby the magnetisation is periodically returned to some

* Corresponding author.
E-mail address: Brian.Hills@bbsrc.ac.uk (B. Hills).

1090-7807/$ - see front matter © 2010 Elsevier Inc. All rights reserved.
doi:10.1016/j.jmr.2010.05.003

value that can be called, M_s. In this steady-state the magnetisation will have lost all memory of its initial state and can be regarded as being at equilibrium at a new spin temperature that differs from the laboratory value [12]. The simplest pulse sequence for achieving this comprises a train of equally spaced 180° pulses such that, starting from the equilibrium state, the longitudinal magnetisation eventually enters a steady-state with a saw-tooth pattern of inversion and recovery. This steady-state situation is straightforward to calculate with the well-known expression derived from the Bloch equations for the recovery of single exponential relaxation from an initial state $M(0)$,

$$M(t) = M_\infty + [M(0) - M_\infty]\exp(-R_1 t) \quad (1)$$

Here R_1 is the longitudinal relaxation rate, $1/T_1$, and M_∞ is the equilibrium longitudinal magnetisation. Consider the situation in the steady-state created by a train of 180° pulses with a spacing, t_e. At a time t_e after a 180° inversion pulse we have an increase in the longitudinal magnetisation from the inverted steady-state, $-M_s$, to a new value,

$$M(t_e) = M_\infty - (M_s + M_\infty)exp(-R_1 t_e) \quad (2)$$

This magnetisation is flipped by the next 180° pulse and the magnetisation now increases again such that after another t_e period we have,

$$M(2t_e) = M_\infty + [-2M_\infty + (M_s + M_\infty)exp(-R_1 t_e)]\exp(-R_1 t_e) \quad (3)$$

But in the steady-state $M(t_e) = M(2t_e)$, so equating (2) and (3) gives

$$m = \{1 - \exp(-R_1 t_e)\}/\{1 + \exp(-R_1 t_e)\} \quad (4)$$

where t_e is the pulse spacing, and m is the steady-state magnetisation, M_s, divided by the equilibrium magnetisation, M_∞. The modulus of m is plotted as a function of t_e for several values of T_1 in Fig. 1 and shows that there is no maximum or minimum and that the steady-state magnetisation approaches zero (or is 'nulled') only at very short pulse spacings such that $t_e \ll T_1$. Fig. 2 shows how a two-dimensional T_1–T_2-spectrum can be acquired by combining the steady-state situation described by Eq. (4) with a standard CPMG pulse sequence. The first box in Fig. 2 represents the standard

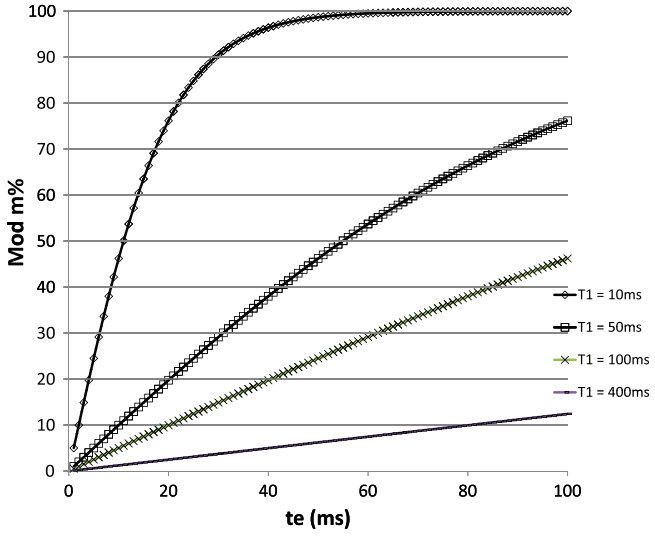

Fig. 1. The theoretical dependence of the steady-state magnetisation ratio M_s/M_∞ (i.e. modulus m%) on echo spacing, t_e, for four values of the longitudinal relaxation time, T_1, using the periodic pulse sequence in Fig. 2, having separate acquisition and preparation and a single pulse spacing (t_e). Curves have been calculated using Eq. (4).

CPMG sequence starting with equilibrium longitudinal magnetisation and acquired with a short echo spacing, 2τ, typically a few hundred microseconds. This "acquisition" CPMG sequence uses sufficient spin-echoes to reach the base-line and thereby accurately characterises the transverse relaxation for both long and short T_2 components. By the end of this CPMG echo train the longitudinal magnetisation will have attained a steady-state value given by Eq. (4) with 2τ replacing t_e. Because $R_1\tau \ll 1$ for all transverse relaxation times longer than a few milliseconds this steady-state magnetisation can be neglected. This initial "acquisition" CPMG pulse sequence is followed by a "preparation" or "dummy" sequence comprising a train of 180° inversion pulses with a longer pulse spacing, t_e, but with no data acquisition. The purpose of this preparation sequence is to establish a new steady-state in the longitudinal magnetisation, as described by Eq. (4) for each T_1 component in the sample. This preparation sequence is followed by a repeat of the first "acquisition" CPMG sequence obtained by replacing one of the preparation 180° pulses with a 90° pulse and using the same echo spacing, 2τ, and number of spin-echoes as in the first acquisition CPMG. The bottom part of Fig. 2 illustrates the time-evolution of the envelope of the longitudinal magnetisation for the sequence ignoring the saw-tooth pattern created by the chain of 180^0 inversion pulses. Analysing the echo decay envelopes from the first and second "acquisition" CPMG sequences with a standard deconvolution programme, such as UPEN [14,15] gives two, one-dimensional T_2 spectra comprising discrete peaks such as those shown in Fig. 3(top). The two spectra will, ideally, have the same T_2-peak positions but the areas of the peaks will, in general, differ because the first was acquired starting with equilibrium magnetisation, the second with steady-state magnetisation in each of the components contributing to the peaks in the T_2-spectrum. The ratio of corresponding peak areas in the two T_2 spectra is therefore a direct measurement of the normalised, steady-state magnetisation, m, for each T_2-peak so the T_1 characterising a particular T_2-peak can be calculated using Eq. (4) and the results displayed as a discrete two-dimensional T_1–T_2-spectrum, such as that illustrated in Fig. 3 (bottom). As Eq. (4) shows, the steady-state magnetisation for a T_2-peak characterised by a long T_1 is severely suppressed at short echo spacing so requires a long, t_e, in the preparation CPMG part of the sequence to give a measurable peak area. For this reason it may be necessary to run the pulse sequence several times with increasingly long preparation echo spacings, t_e, to properly characterise both the short and long T_1 components in the sample. In principle this can be done in a fast single-shot sequence by simply extending the pulse sequence to include the desired set of preparation t_e values. The fact that the steady-state magnetisation of components with long T_1's is suppressed more than those with short T_1's can be an advantage in some water-rich biological samples because it suppresses the water peak and enhances the more interesting solute and biopolymer peaks in the spectrum. Of course, any prior knowledge of the likely range of T_1 values in the sample will allow a suitable choice of preparation echo spacing(s) to be estimated with Eq. (4).

If there are two peaks with the same T_2 but different T_1's, the separate T_1's would require measurements at two different t_e so that the separate T_1's can be obtained by solving the pair of simultaneous equations comprising Eq. (1) for two sets of t_e and T_1 values. It should also be noted that Eq. (1) neglects the possible effects of magnetisation transfer on the steady-state magnetisation established in a sample having several proton pools exchanging longitudinal magnetisation. This aspect will be the subject of future theoretical analysis but lies outside the scope of this initial development.

The same periodic FLOP–T_1–T_2 methodology can be extended to trains of periodically repeating 180 pulses having different pulse spacings. Consider, for example, the situation when the preparation

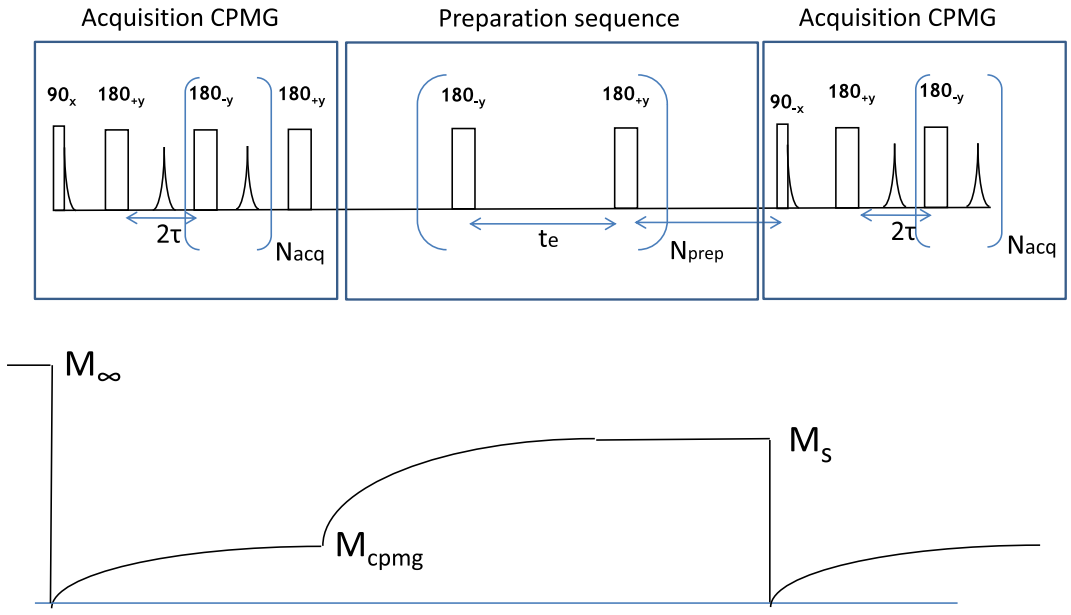

Fig. 2. (Top): The general scheme for the periodic pulse sequences. The acquisition CPMG boxes would normally use a short echo spacing, 2τ, and a large number of echoes, N_{acq}, to reach the base-line. The preparation sequence would use a longer echo spacing, t_e, and sufficient pulses, N_{prep}, to establish a steady-state as described by Eq. (4). (Bottom): An illustration of the associated changes in the longitudinal magnetisation which would have a saw-tooth pattern from the 180° inversion pulses but only the envelope is illustrated.

sequence in Fig. 2 comprises the periodically repeated pattern of pulse spacings $\{-t_2-t_3-\}_N$ where N is the number of repetitions. In this case the steady-state condition is given as (12),

$$m = \{-1 + 2\exp[-R_1 t_3] - \exp[-R_1(t_2 + t_3)]\}/\{1 - \exp[-R_1(t_2 + t_3)]\} \quad (5)$$

As before, a measurement of m, for known values of t_2 and t_3, allows determination of the longitudinal relaxation T_1 and the construction of a discrete T_1–T_2-spectrum. However, unlike the equal pulse spacing case, the steady-state null condition is non-trivial and is obtained by putting m to zero when

$$t_{3\text{null}} = T_1 \text{Ln}[2 - \exp(-R_1 t_2)]. \quad (6)$$

In this case the suppression of the longitudinal magnetisation can be taken all the way to the null point at finite values of t_2 and t_3 which is especially useful if one high intensity relaxation peak dominates the T_2-spectrum and needs to be suppressed. Fig. 4 shows a plot of the modulus of m as a function of t_3 for a fixed t_2 of 10 ms for several values of T_1. Note that, in this case, m is rather insensitive to changes in T_1 so that this particular sequence is less useful for T_1 determinations than the constant t_e sequence. Because of this it is worth progressing to the next level of complexity by analysing the periodically repeated pattern of pulse spacings $\{-t_3-t_3-t_2-\}_N$. As we shall show in the next section, this is also one of the simplest sequences that allows integration of the preparation and acquisition modes. The expression for the steady-state magnetisation ratio, m ($=M_s/M_\infty$), for this periodic sequence can be shown to be (12),

$$m = [C + 1]/[1 + \exp\{-R_1(2t_3 + t_2)\}] \quad (7)$$

where

$$C = [-2 + [2 - \exp(-R_1 t_3)]\exp(-R_1 t_3)]\exp(-R_1 t_2) \quad (8)$$

According to Eq. (7) a non-trivial null point can be obtained by solving the equation $C = -1$ and gives,

$$t_{3\text{null}} = -T_1 \text{Ln}\{1 - [\exp(R_1 t_2) - 1]^{0.5}\} \quad (9)$$

where it has been assumed that t_2 is fixed and t_3 is the variable.

The modulus of the function $m(t_2, t_3)$ in Eq. (7) is plotted as a function of t_3 in Fig. 5 for t_2 values of 10 ms (Fig. 5a) and 30 ms (Fig. 5b) and for several values of T_1. It is interesting that Fig. 5a shows a maximum for t_3 values less than the null point and that this part of the curve is sensitive to T_1 so provides a second method for determination of T_1 and of the discrete T_1–T_2-spectrum.

2.2. Theoretical analysis of periodic FLOP sequences with combined preparation and acquisition

The FLOP–T_1–T_2 sequences discussed in Section 2.1 are fast, single-shot sequences but they are not optimised for maximum speed because the acquisition and preparation parts of the sequence are separated and CPMG acquisition part leaves the system with zero transverse magnetisation and a near-zero steady-state longitudinal magnetisation, as determined by Eq. (4). Establishing a new steady-state after the CPMG acquisition sequence therefore requires a long train of 180° pulses in the preparation part of the sequence. One can attempt to rectify this situation by combining the acquisition and preparation modes into a single repeating pulse sequence. The case of equal pulse spacing is trivial, in the sense that it is just two CPMG sequences joined together each with a pulse spacing t_e. The first CPMG sequence starts with equilibrium magnetisation whereas the second starts from steady-state magnetisation as determined by Eq. (4). Deconvoluting each CPMG sequence with, for example, the UPEN software package [14,15] gives two discrete T_2 spectra and the steady-state magnetisation, m, of each T_2-peak is obtained as the ratio of corresponding peak areas and, via Eq. (4), gives the T_1 of each T_2-peak and a discrete T_1–T_2-spectrum. The approach is therefore very similar to that described in Fig. 2 but has the advantage that the first CPMG sequence starting with equilibrium magnetisation also acts as a preparation sequence for the steady-state longitudinal magnetisation. It is therefore intrinsically faster than the method in Section 2.1 with equal pulse spacings. However, to observe significant signal in the second CPMG, long echo times, t_e, are needed otherwise the condition $t_e R_1 \ll 1$ means there is no observable steady-state magnetisation. The long echo

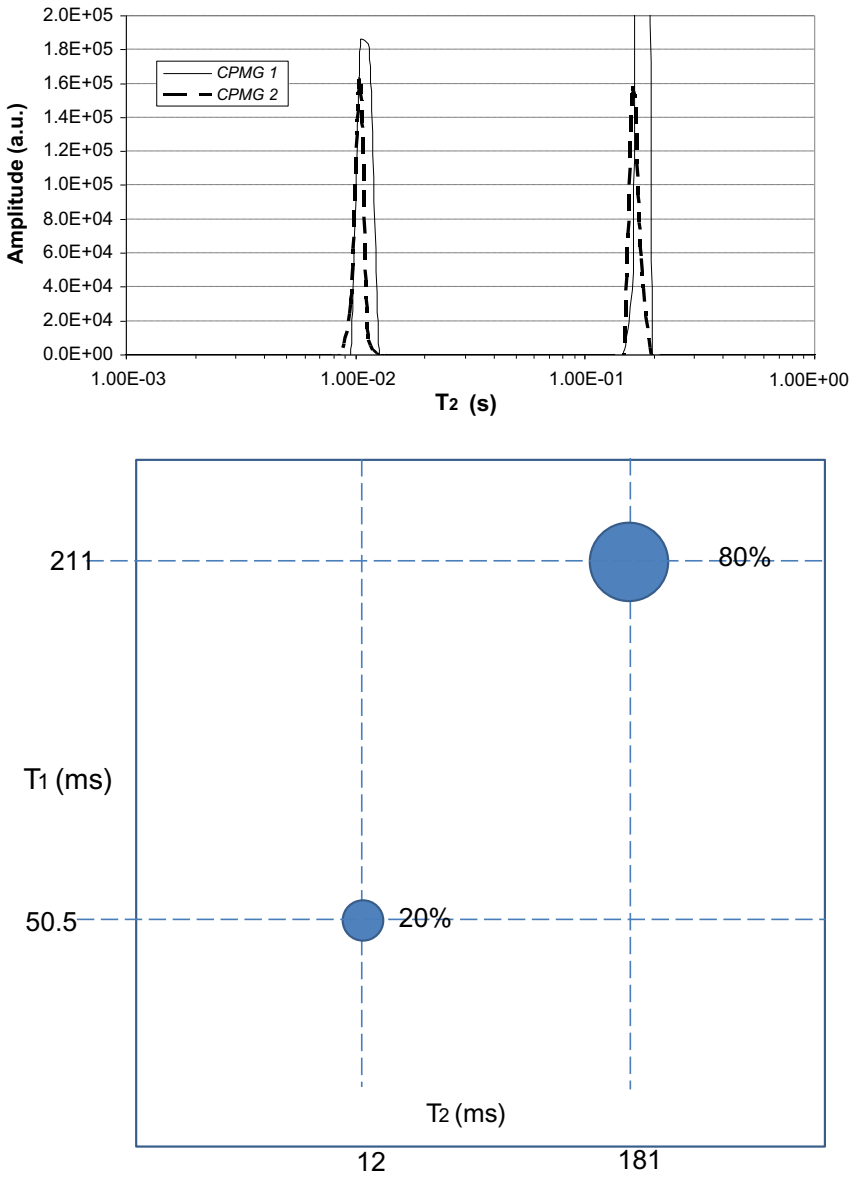

Fig. 3. The methodology for measuring a discrete T_1–T_2-spectrum using the periodic sequence in Fig. 2 with a single echo spacing (t_e) and separate preparation and acquisition sequences. The spectra correspond to the results for double-doped water in Table 1 with $t_e = 60$ ms. The T_2 spectra for the equilibrium and steady-state magnetisations for the two acquisition CPMG sequences in Fig. 2 are shown (top) and the area ratio for each T_2-peak gives m% for each peak. This, together with Eq. (4) gives the T_1 value for each T_2-peak, presented as a discrete T_1–T_2-spectrum (bottom).

spacing therefore has the disadvantage that components with short T_2 are poorly characterised.

An attempt can be made to remove this last limitation using unequal pulse spacings However it is impossible to create an combined preparation-acquisition sequence based on the $-[-t_2-t_3-]_N$ – repeating unit when $t_3 \neq t_2$ because this condition is incompatible with the requirement that the rephasing time equals the dephasing time for spin-echo formation. A repeatable pattern of spin-echoes cannot therefore be formed with this sequence. Some thought shows that the next simplest periodic FLOP–T_1–T_2 sequence with combined acquisition and preparation is based on the repeating unit $[-t_{3a}-t_{3a}-t_2-t_{3b}-t_{3b}-t_2-]$. This appears to be unnecessarily complicated but it is actually one of the simplest that satisfies the four requirements that (1) the unit can be repeated periodically, (2) the longitudinal magnetisation at the beginning and end of the repeating unit is the same so that a steady-state is established in the longitudinal magnetisation, and (3) that the spin-echoes in the transverse magnetisation form a-periodic repeating pattern. The repeating pattern $[-t_3-t_3-t_2-]$ gives a repeatable pattern of spin-echoes but fails on criterion (1) because the whole pattern is not repeatable. This can be seen in Fig. 6 where the non-repeatability arises because the first and last 180 pulses in the unit $[-t_3-t_3-t_2-]$ cause inversions in opposite directions. This directional problem can be overcome by joining two of the $[-t_3-t_3-t_2-]$ units together so that the repeating unit is $[-t_{3a}-t_{3a}-t_2-t_{3b}-t_{3b}-t_2-]$ which is the sequence illustrated in Fig. 6. For generality it is not necessary to assume that t_{3a} equals t_{3b}, although, as we shall demonstrate, the extraction of a discrete T_1–T_2 relaxation spectrum is a lot easier if they are made equal. For simplicity we have centred the spin echo in the middle of the t_2 periods so that it is necessary that t_{3a}, $t_{3b} > t_2$ to maintain a repeatable pattern of spin-echoes.

Fig. 6 assumes that the sequence has already been repeated sufficient times that a steady-state has evolved from the initial

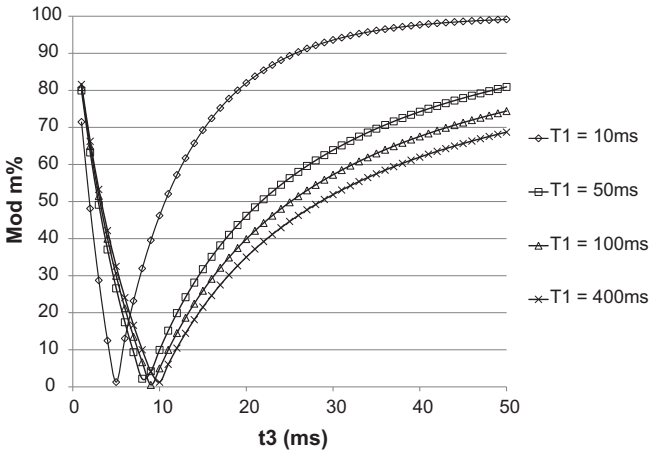

Fig. 4. The theoretical dependence of the steady-state magnetisation ratio (modulus m%) on echo spacing, t_3 for four values of the longitudinal relaxation time, T_1, using the periodic pulse sequence $-t_2-t_3-$ having separate acquisition and preparation. Curves have been calculated using Eq. (5) for a fixed t_2 of 10 ms.

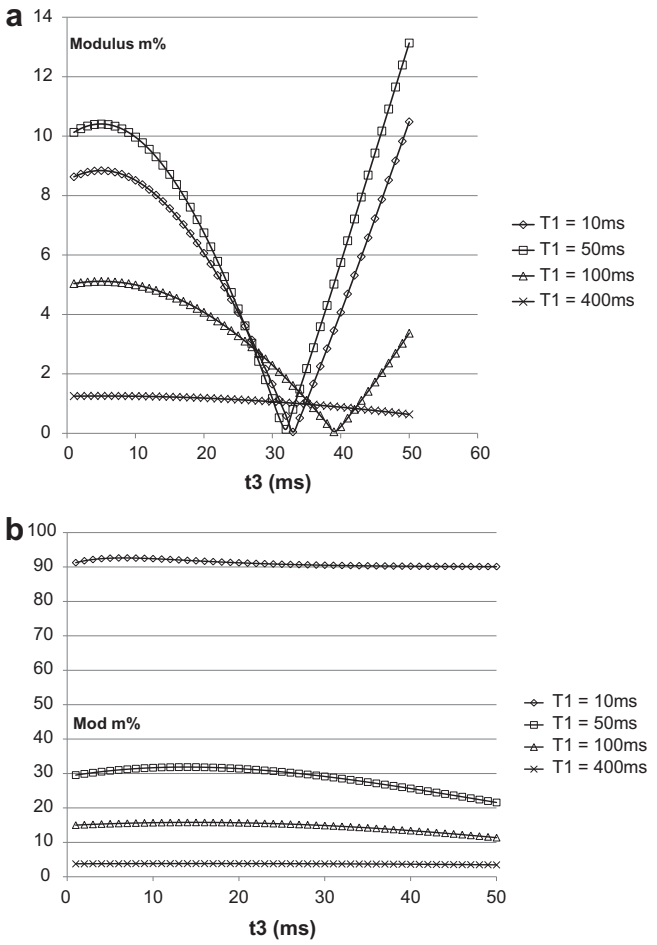

Fig. 5. The theoretical dependence of the steady-state magnetisation ratio (modulus m%) on echo spacing, t_3 for four values of the longitudinal relaxation time, T_1, using the periodic pulse sequence $-t_3-t_3-t_2-$ having separate acquisition and preparation. Curves have been calculated using Eq. (7) for a fixed t_2 of (a) 10 ms and (b) 30 ms.

equilibrium magnetisation. After the steady-state has been established a train of spin-echoes can be initiated by locating a 90° pulse at a time $0.5t_2$ after the 180° pulse as indicated by the symbol 90 in Fig. 6 (where it replaces the spin echo). Each 90-degree initiated echo train will continue until transverse relaxation has caused the echo amplitude to decay into the base-line. A new CPMG echo train can then be initiated by repeating the 90 pulse in another repeated unit in the periodic pattern. Although the 90 pulse removes the steady-state longitudinal magnetisation the repeated train of 180° pulses soon re-establishes the steady-state in the longitudinal magnetisation before the next 90 pulse. In this way trains of decaying spin-echoes can be acquired and used to characterise the T_2 relaxations. Not all the spin-echoes need be acquired and, for convenience, the spin-echoes labelled AQ will give an equal echo spacing of $2(t_{3a} + t_{3b})$. Each echo decay envelop can be deconvoluted in the conventional way using UPEN into a one-dimensional T_2-spectrum. However, to extract the T_1 information it is necessary to analyse the dependence of the steady-state magnetisation, M_s, in Fig. 6 on the pulse spacings t_2, t_{3a} and t_{3b}. This is done in Appendix A which shows that

$$m = (1 + B)/(1 - A) \tag{10}$$

where as before, we have defined the normalised steady-state magnetisation, m, as the ratio M_s/M_∞ and M_s is the steady-state magnetisation indicated in the lower half of Fig. 6. The terms A and B are

$$A = \exp[-R_1 2(t_{3a} + t_{3b} + t_2)] \tag{11}$$

$$\begin{aligned} B = {} & [-2 - [-2 - [-2 - [-2 - [-2 + \exp(-R_1 t_{3a})] \\ & \times \exp(-R_1 t_{3a})] \exp(-R_1 t_2)] exp(-R_1 t_{3b})] \\ & \times \exp(-R_1 t_{3b})] exp(-R_1 t_2) \end{aligned} \tag{12}$$

The numerical solution of the general sequence in the steady-state with t_{3a} set equal to t_{3b} shows that the longitudinal magnetisation at the midpoint, (i.e. the magnetisation after the first t_2 period in Fig. 1) is equal to M_s. This is not an obvious result because the two t_2 periods are not equivalent because one involves negative magnetisation, the other positive magnetisation. Nevertheless this numerical result simplifies the analytical solution considerably because it shows it is only necessary to solve for the steady-state after the t_3–t_3–t_2 sequence which is half the repeating unit t_3–t_3–t_2–t_3–t_3–t_2. This has already been done in Section 2.1 resulting in Eqs. (7) and (9) and illustrated in Figs. 5a and b. Reference to Fig. 6 shows that the measured steady-state magnetisation at the position of the 90° pulse, $M(t_2/2)$, differs slightly from M_s but it is easy to show that

$$M(t_2/2)/M_\infty = 1 - [m + 1] exp(-R_1 t_2/2) \tag{13}$$

Measurement of $M(t_2/2)/M_\infty$ for known values of t_2 and t_3 therefore allows the T_1 to be calculated from Eqs. (10) and (13) for each component peak in the T_2-spectrum and the discrete T_1–T_2-spectrum to be constructed.

Fig. 5 illustrates one major limitation with this combined [$-t_3$–t_3–t_2–t_3–t_3–t_2–] sequence, namely that measureable values of the steady-state magnetisation, m, especially for the long T_1 components, still require quite long pulse spacings, t_2, which also means a long t_3 to satisfy the condition $t_3 > t_2$. So despite its increased complexity, this pulse sequence still suffers from the disadvantage that short T_2 components will be difficult to characterise. This is not a limitation in Section 2.1 where the acquisition and preparation steps are separated.

2.3. The magic-SPACE box sequence

Because the periodic FLOP–T_1–T_2 sequences are single-shot and use the steady-state there is no need to wait a recycle delay of $5T_1$ for recovery of longitudinal magnetisation, which is the case with the conventional inversion recovery T_1–T_2 acquisition. They are therefore fast sequences which makes them particularly suitable

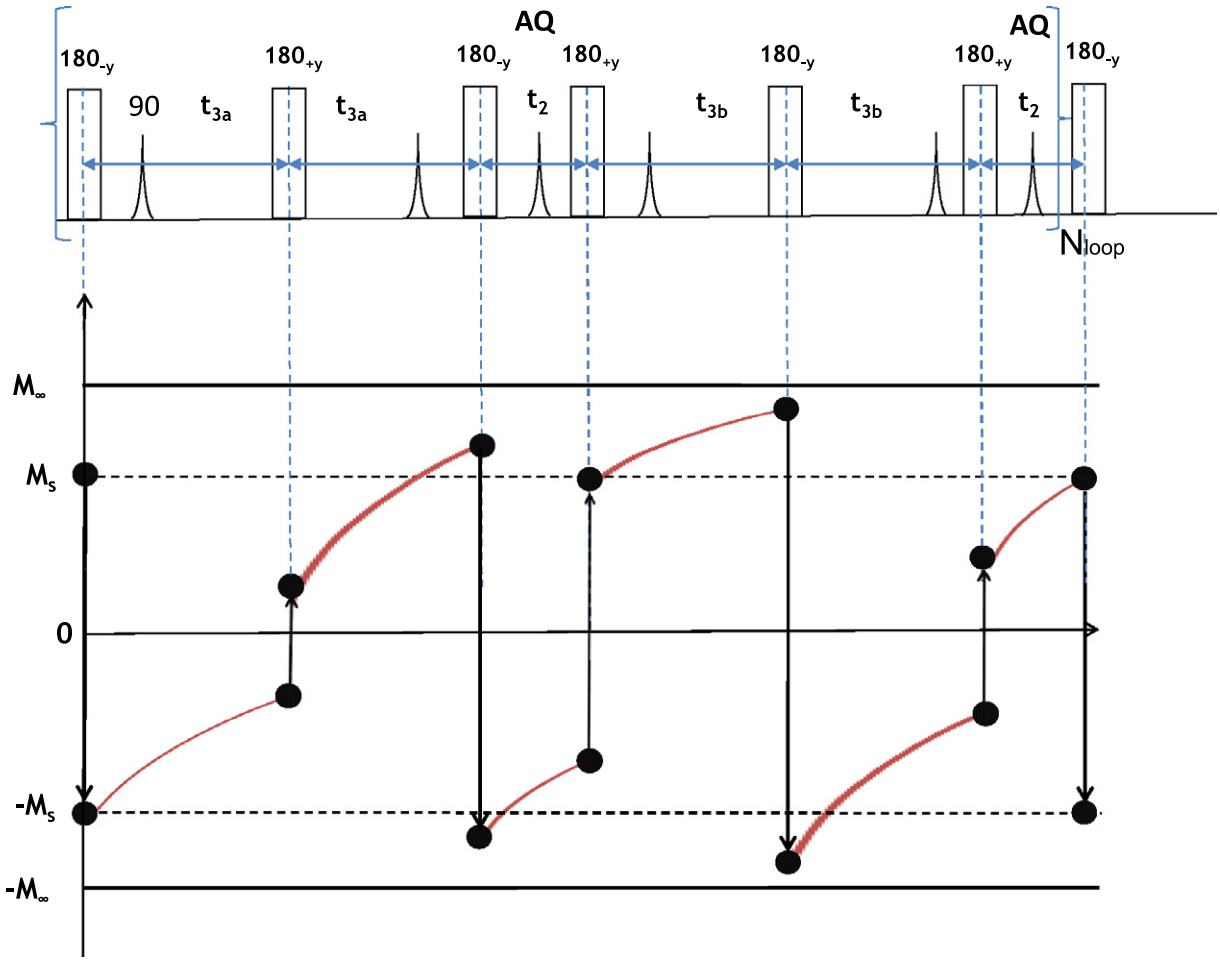

Fig. 6. The pulse sequence for combined acquisition and preparation based on the repeated unit $-[t_{3a}-t_{3a}-t_2-t_{3b}-t_{3b}-t_2]-$. A schematic of the time course of the longitudinal steady-state magnetisation is shown below the pulse sequence. The AQ symbol denotes those spin-echoes that are most conveniently used for signal acquisition. A steady-state has been assumed and the echo train is triggered when a 90° pulse replaces the spin echo as indicated.

for rapid acquisition of discrete T_1–T_2 spectra from particular tissues or volumes of interest (VOI) in clinical MRI. However, in such clinical applications it is necessary to remove all signals from outside the VOI. To do this each FLOP–T_1–T_2 sequence can be started with the conventional SPACE sequence (4). However, this alone is insufficient to confine the acquired signal to the VOI because the FLOP–T_1–T_2 sequences soon re-establish the steady-state magnetisation M_s throughout the whole sample. It is therefore necessary to insert additional pulses that periodically destroy the magnetisation outside the VOI. This has to be done in such a way that the steady-state longitudinal magnetisation within the VOI is preserved while maintaining any echo train in the transverse magnetisation within the VOI. Fig. 7 shows a schematic of a sequence that we have called the magic-SPACE-box that achieves this aim and which can be inserted periodically between any two hard 180° pulses in the FLOP–T_1–T_2 sequences. As Fig. 7 illustrates, the magic-SPACE-box not only destroys all longitudinal magnetisation outside the VOI but it also refocuses the transverse component of the magnetisation within the VOI as a negative echo. This negative echo can be corrected in the data processing stage but will also be reversed by the next application of the magic-SPACE box. The longitudinal magnetisation within the VOI is converted to transverse magnetisation by the first 90 pulse then refocused by the selective 180 and returned as longitudinal magnetisation by the second 90 pulse. It is therefore essentially "frozen" between the two 90 pulses, though it suffers a slight attenuation of $\exp(-t_2/T_2)$. This minor perturbation is removed after a few more inversion pulses. For simplicity Fig. 7 only shows the magic-SPACE box sequence for a one-dimensional "slice" but it can, of course, be generalised to three dimensions with three selective 180° pulses each in a gradient with an orthogonal direction. Of course the longitudinal attenuation is then $\exp(-3t_2/T_2)$.

2.4. Aperiodic FLASH-FLOP T_1–T_2 sequences

The periodic sequences discussed in previous sections all require that a steady-state in the longitudinal magnetisation is established by periodic repetition. Even when the acquisition and preparation modes are combined into a single sequence, as in Section 2.2, it nevertheless takes a finite time to establish the steady-state. In this section we therefore explore the possibility of acquiring the T_1–T_2-spectrum directly in an ultrafast, non-periodic acquisition protocol. In principle this can be done using the pulse sequence in Fig. 8, which can be called the aperiodic FLASH-FLOP–T_1–T_2 sequence. As its name implies, the 180° pulse spacings in Fig. 8 do not repeat themselves and need to be individually calculated. The Fast Low-Angle SHot (FLASH) methodology [16] has also been incorporated by creating transverse magnetisation with θ-degree pulses where $\theta < 90$ so that the whole sequence can be run in a single shot. The intrinsic a-periodic nature of the FLASH-FLOP T_1–T_2 sequence arises because it is combined with a variable inversion recovery time (t_1) which gives a variable initial magnetisation, $M(t_1)$, which then

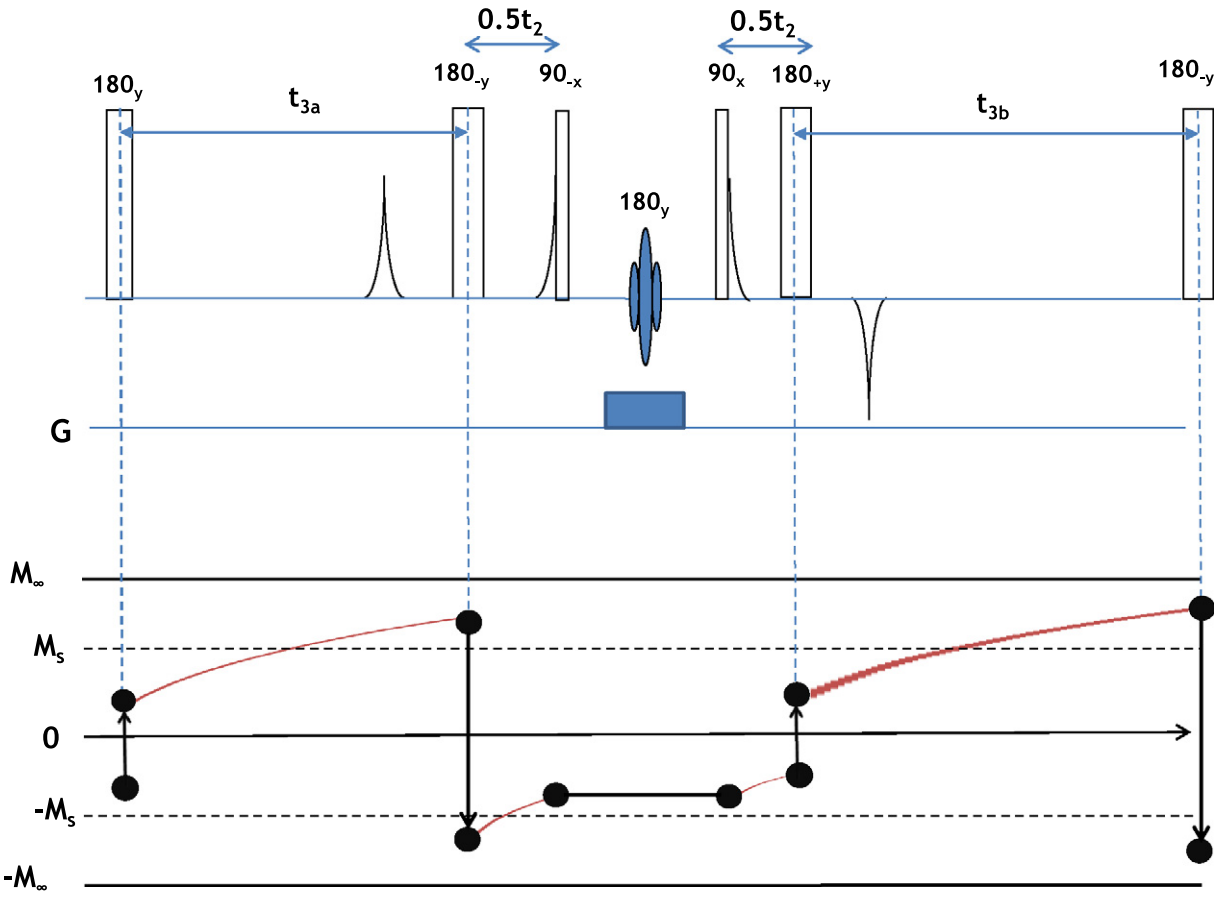

Fig. 7. The magic-SPACE box pulse sequence for periodically destroying magnetisation outside the VOI while preserving longitudinal and transverse magnetisation within it. A schematic of the time course of the longitudinal steady-state magnetisation is shown below the pulse sequence.

determines the subsequent time-evolution of the longitudinal magnetisation which has to be matched with the requirement that the refocusing time has to equal the dephasing time for spin-echo formation in the transverse magnetisation.

The first delay time, t_1, in Fig. 8 is normally read off a list of logarithmically-spaced inversion recovery times chosen to measure T_1 in the first time dimension. The time period t_2 between the theta degree pulse and the next 180° pulse is a matter of choice but should be as short as possible to avoid unnecessarily long spin echo times in the rest of the acquisition. The time period t_3 is also a matter of choice, subject only to the constraint that it needs to be longer than t_2 so that the first spin echo can be acquired between the second and third 180° pulses. t_4 is therefore the first non-arbitrary time period and must be calculated so that the longitudinal magnetisation after the t_4 period equals the longitudinal magnetisation after the t_2 period (see Fig. 8). This logic is continued with subsequent time periods. t_5 is arbitrary apart from the constraints that it should be as short as possible yet longer than t_4 so that the third echo can be acquired before the next 180° pulse. t_6 is then calculated so that once again the residual longitudinal magnetisation after the t_6 period equals the magnetisation after the t_2 and t_4 periods and so on. As Fig. 8 illustrates, these requirements mean that the spin-echoes occur in pairs either side of alternative 180° pulses and that the spacing between these echo pairs progressively increases. The whole echo train is continued until the echo amplitude is in the noise (base-line) when any small residual transverse magnetisation is destroyed by a short spoiler gradient pulse timed so that it coincides with the time when the residual longitudinal magnetisation is once again recovered to the value it had after the t_2 time period. The whole spin echo sequence can then be repeated with the next inversion recovery delay time, t_1, and initiated with the next theta degree pulse, remembering that the inversion recovery time now includes the t_1 period from the previous cycles. This means that the whole T_1–T_2 acquisition can be programmed as an ultrafast single-shot sequence where the number of data points in the first inversion recovery time dimension is determined by the total number of theta degree pulses; while the number of acquired spin-echoes in the second time dimension will vary with t_1 and be limited by the need to fit all the increasing echo times in a total time of the order of $5T_2$. The price paid for the increased acquisition speed is therefore not just the loss of signal/noise because a theta degree pulse, rather than a 90° pulse, has been used but also in a reduced number of spin-echoes and inversion recovery times. The later problem can be alleviated to some extent by post data processing, and this will be discussed in Section 2.4.2. In the next section we present the calculation of the various delay times in the sequence.

2.4.1. Calculation of the a-periodic FLASH-FLOP–T_1–T_2 delay times

Repeated application of the inversion recovery Eq. (1) shows that the magnetisation after an odd time period, t_{2n+1} ($n \geqslant 1$) in the pulse sequence in Fig. 8 is given as

$$M^{-}(t_{2n+1}) = M_{\infty} + 2M_{\infty}[-1 + (1 + A_{2n-1})\exp(-R_1 t_{2n})] \times \exp(-R_1 t_{2n+1}) \quad (n \geqslant 1) \tag{14}$$

where

$$A_{2n-1} = [-1 + (1 + A_{2n-3})\exp(-R_1 t_{2n-2})]\exp(-R_1 t_{2n-1}) \quad (n \geqslant 1) \tag{15}$$

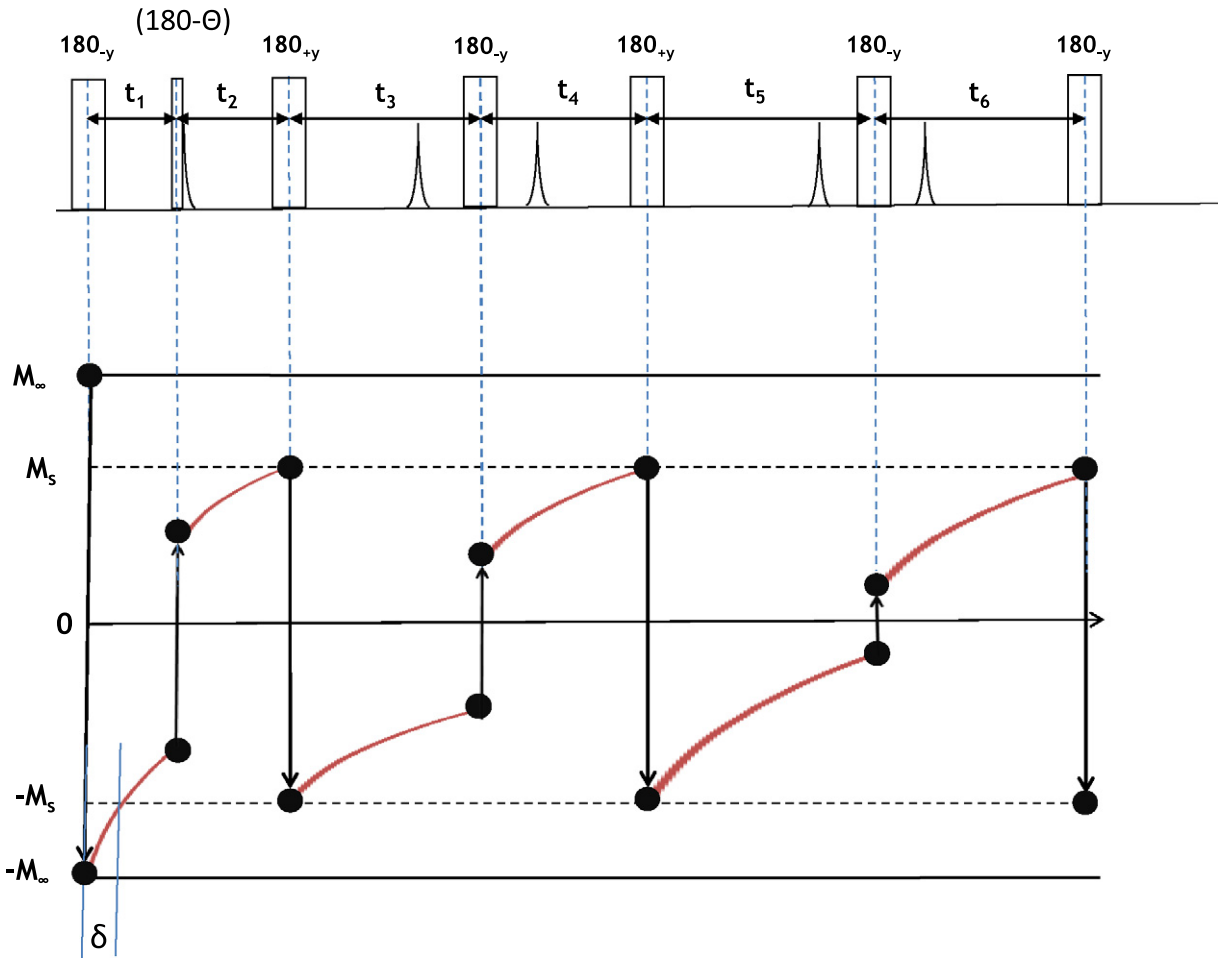

Fig. 8. The a-periodic FLASH-FLOP pulse sequence (top) together with a schematic of the time-evolution of the longitudinal magnetisation (bottom).

and

$$A_3 = [-1 + (1 - \exp(-R_1 t_1)]\exp(-R_1 t_2)]\exp(-R_1 t_3) \quad (16)$$

The negative superscript in $M^-(t_{2n+1})$ denotes that the magnetisation is calculated before the 180° pulse at the end of the time period t_{2n+1}. A 180° pulse inverts the longitudinal magnetisation so that the magnetisation after the pulse, $M^+(t_{2n+1})$, is

$$M^+(t_{2n+1}) = -M^-(t_{2n+1}) \quad (17)$$

Similarly the magnetisation after an even time period can be shown to be

$$M^-(t_{2n}) = M_\infty - 2M_\infty[1 + (-1 + B_{2n-2})\exp(-R_1 t_{2n-1})] \times \exp(-R_1 t_{2n}) \quad (n \geqslant 1) \quad (18)$$

where

$$B_{2n-2} = [1 + (-1 + B_{2n-4})\exp(-R_1 t_{2n-3})]\exp(-R_1 t_{2n-2}) \quad (19)$$

and

$$B_2 = (1 - \exp(-R_1 t_1))\exp(-R_1 t_2) \quad (20)$$

with $B_0 = 0$. The delay times are now straightforward to calculate from the requirement that, before the T_1 null point, $M^-(t_2) = M^-(t_{2n})$ for $n \geqslant 1$. This gives

$$t_{2n+2} = t_{2n} + R_1^{-1} Ln\{1 + [-1 + B_{2n}]\exp(-R_1 t_{2n+1})\} - R_1^{-1} Ln\{1 + [-1 + B_{2n-2}]\exp(-R_1 t_{2n-1})\} \quad (n \geqslant 1) \quad (21)$$

The time delay t_1 is determined by the list of desired logarithmically-spaced inversion recovery times, chosen to cover the range of sample T_1's. As already mentioned, the delay time t_2 is a matter of choice, but needs to be kept as short as possible to maximise the number of spin-echoes characterising the transverse relaxation. t_3 is also a matter of choice but needs to be longer than t_2 so the first spin-echo falls within the first t_3 time period (see Fig. 8). t_4 and is then calculated from Eq. (21). t_5 is also arbitrary but again needs to be $\geqslant t_4$ so the spin-echo falls within the t_5 period. For simplicity the t_5 can be set equal to t_4 and, in general, t_{2n+1} can be set equal to t_{2n}, for $n \geqslant 2$.

At the end of a spin-echo train, after the echo decay envelop has decayed into the background noise, the whole sequence can be immediately repeated with the next inversion recovery delay time, t_1, and a new set of time delays calculated with the above equations. However because the sequence ends with the magnetisation $M_s(=M(t_1 + t_2)$ the next inversion recovery time in the list is not t_1 but $(t_1 - \delta)$ where δ is the time required for $-M_\infty$ to recover to $-M_s$ of the previous acquisition cycle and is easily calculated as

$$\delta = -T_1 Ln[1 - \{\exp(-R_1 t_1\}\exp(-R_1 t_2)]. \quad (22)$$

This delay time is indicated in Fig. 8.

The situation after the null point is slightly different because the sequence of the time periods associated with inverted longitudinal magnetisation is changed. The time periods t_{2n} $(n \geqslant 2)$ must now be calculated and are determined by the requirement that $M^-(t_{2n+2}) = M^-(t_{2n})$ for $n \geqslant 2$, with $M^-(t_4) = M^-(t_1)$. A similar calcu-

lation to that presented in Section 2.2 yields the same Eq. (21) for the pulse spacing but with the new condition that $n \geqslant 2$ and

$$t_4 = t_1 + R_1^{-1} Ln\{1 + A_3\} \tag{23}$$

2.4.2. Intrapolation of the FLASH-FLOP spin echo data

The equations in Section 2.4.1 can be used to construct a two-dimensional matrix of time delays (t_1, τ_2) and associated spin echo amplitudes, $M(t_1, \tau_2)$, for each inversion recovery time, t_1, and spin echo time, τ_2 in the aperiodic FLASH-FLOP–T_1–T_2 sequence. Fig. 8 shows that the spin-echoes occur in pairs centred either side of alternate 180° refocusing pulses. The echo positions are easily calculated by noting that the separation, TE_n between the nth pair of spin-echoes is

$$TE_n = 2 \sum_{m=0}^{(2n-2)} (-1)^m t_{2n-m+1} \tag{24}$$

While the nth such echo pair is centred at the time T_{centre} given as

$$T_{centre} = \sum_{j=1}^{(2n+1)} t_j \tag{25}$$

so that the spin-echoes are located at

$$\tau_2 = (T_{centre} \pm 0.5TE_n) \text{ for } n \geqslant 1. \tag{26}$$

Continuous inversion recovery T_1–T_2 spectra are usually obtained using the fast 2D Inverse Laplace transform algorithm developed by Song and Hurlimann [1,2]. Unfortunately this algorithm assumes that the echo spacings in the second dimension are the same for each inversion recovery delay time, t_1, which is not the case in the aperiodic FLASH-FLOP sequence. It is therefore necessary to convert the data into equally spacing along the T_2 dimension which can be most easily achieved by fitting each experimental echo decay envelope with a multiple exponential function and using the resulting fitting function to calculate the amplitudes of the spin-echoes at a set of echo times that covers the whole decay range and which is the same for each inversion time. This is also an opportunity to increase the digital resolution by artificially increasing the number of spin-echoes. Of course, this intrapolation, like zero-filling, does not improve the intrinsic resolution of the relaxation time spectrum, but it does mean that the fast 2D inverse Laplace algorithm can be used and results in recognisable continuous 2D inversion recovery T_1–T_2 relaxation spectra. The loss of resolution is the price that must be paid for the reduced acquisition times.

The consistency of the FLASH-FLOP–T_1–T_2 protocol was tested with a simulated test sample comprising three equally weighted component T_2's of 50,100 and 600 ms and a single T_1 of 600 ms. In this test, Eqs. (14)–(23) were used to calculate the unequally spaced FLASH-FLOP matrix $M(t_1,\tau_2)$ which was then converted to an equally spaced matrix by intrapolation and input into the standard 2D inverse Laplace transform resulting in the continuous T_1–T_2-spectrum in Fig. 9 which agrees moderately well with the input relaxation times and percentages.

Although the aperiodic FLASH-FLOP–T_1–T_2 sequence is fast and gives continuous, rather than discrete, T_1–T_2 spectra, it suffers from several major disadvantages compared to the periodic sequences. It is computationally intensive and the requirement for ever increasing echo spacings means that the paucity of echoes can be severely limiting. Moreover one would expect distortion in the T_1 dimension because the pulse spacings calculated in Eqs. (21)–(23) are all derived for a single T_1, and will not, therefore, be optimum for all the T_1 peaks in a sample having several different T_1's. This was not obvious in the simulated test result because all the peaks had the same T_1.

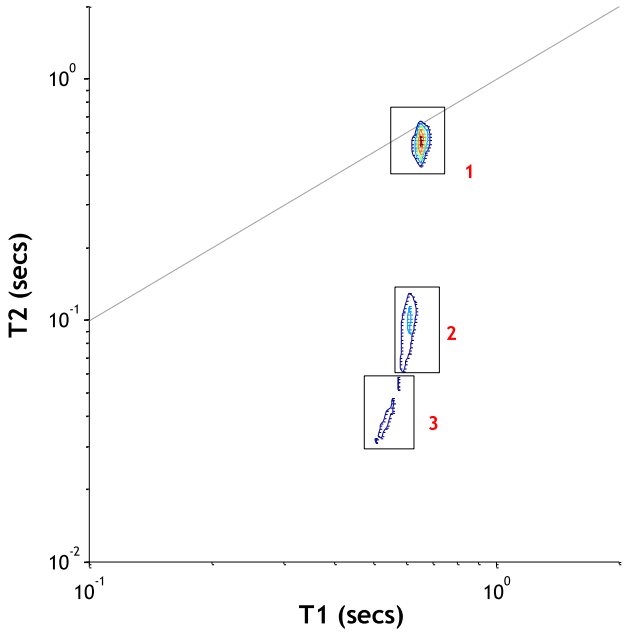

Fig. 9. The calculated T_1–T_2-spectrum for a sample comprising three components each with a T_1 of 600 ms and T_2's of 50,100 and 600 ms in equal proportion. The spectrum has been calculated using equations in Section 2.4.1 for the aperiodic pulse sequence followed by intrapolation (Section 2.4.2) and 2D inverse Laplace transformation. The resulting (T_1, T_2, %) of each peak in the resulting simulated spectrum are peak 1: (650, 556, 39%); peak 2: (610, 102, 39%); peak 3: (537, 39, 22.5%).

3. Materials and method

All measurements were undertaken on an unshimmed Resonance Instruments DRX bench-top spectrometer operating at 23.4 MHz and equipped with pulsed field gradients. The sequences were tested using a phantom sample comprising concentric NMR tubes containing two samples of doped water characterised by (T_2, T_1) values of (12.1, 58.6) and (181, 233.5) ms, respectively. These relaxation times were determined by the conventional CPMG and inversion-recovery methods. A second, more realistic, multicomponent test sample comprised sunflower oil purchased from a local supermarket. This was characterised by two principle relaxation components of (T_{2a} = 10.3 ms; T_{1a} = 56.7 ms) and (T_{2b} = 186 ms; T_{1b} = 243 ms) though the conventional 2D T_1–T_2-spectrum shows evidence for a third low amplitude peak. The non-selective 180° pulse length, as determined by the minimum in the FID amplitude, was 9.7 μs. The CPMG data in the periodic FLOP–T_1–T_2 sequences was deconvoluted into a set of discrete T_2-peaks using the discrete version, EXPON, of the UPEN (Uniform-PENalty Inversion of Multiexponential Decay Data) software package [14,15].

4. Results

Tables 1–3 summarise the test results for the periodic FLOP sequences as applied to the phantom "double doped" water sample. The first sub-table in Table 1 compares the predicted and experimental values of the steady-state magnetisation ratio, m, and the T_1 values where the preparation and acquisition is separated with a single echo time. It can be seen that the experimental steady-state magnetisations are all slightly larger than the predicted values and this leads to the experimental T_1's being systematically lower than the independently measured values. The origin of this systematic error is unknown. Possibilities include a systematic

Table 1
Experimental results for the periodic FLOP sequences with separate preparation and acquisition in Fig. 2 applied to a double-doped water phantom comprising two (T_1; T_2) peaks of (58.6; 12.1) and (233.5; 181) ms. The 90–180 spacing in the acquisition CPMG sequence was 2 ms with 1024 echoes. N_{prep}=128 in the preparation sequence.

	Experimental				Calculated	
	*m*1%	T_{11}	*m*2%	T_{12}	*m*1%	*m*2%
Single echo spacing (t_e). Separate preparation and acquisition. m and T_1 values were obtained by fitting the data with Eq. (4)						
t_e = 10 ms	10.8	46.5	(3.5)	–	8.5	2.15
t_e = 60 ms	53.2	50.5	14.2	211	47.1	12.8
Unequal pulse spacing with repeating pattern, t_3–t_2. Separate preparation and acquisition. m and T_1 values were obtained by fitting the data with Eq. (5).						
t_3 = 1 ms–t_2 = 5 ms	49.7	N/A	50.9	N/A	65.2	66.3
t_3 = 1 ms–t_2 = 10 ms	66.1	N/A	61.7	N/A	80.2	81.4
t_3 = 1 ms–t_2 = 60 ms	97.9	N/A	75.3	N/A	94.8	96.3
Unequal pulse spacing with repeating pattern t_3–t_3–t_2. Separate preparation and acquisition. m and T_1 values were obtained by fitting the data with Eq. (7).						
t_3 = 1 ms; t_2 = 10 ms	10.2	49.5	(6.8)	–	8.6	2.15
t_3 = 1 ms; t_2 = 60 ms	55.15	48.9	17.2	174	47.5	12.8

Table 2
Experimental results for the periodic FLOP sequences with combined preparation and acquisition applied to a double-doped water phantom comprising two (T_1; T_2) peaks of (58.6; 12.1) and (233.5; 181) milliseconds.

	Experimental				Calculated	
	*m*1%	T_{11}	*m*2%	T_{12}	*m*1%	*m*2%
Single echo spacing (t_e). Combined preparation and acquisition. m and T_1 values were obtained by fitting the data with Eq. (4)						
t_e = 5 ms	4.6	54	(2.8)	–	4.26	1.07
t_e = 10 ms	8.2	61	5.4	–	8.5	2.14
t_e = 60 ms	0 (T_2 too short)	–	12.9	231	45.8	12.78
Unequal pulse spacing with repeating pattern, t_3–t_3–t_2. Combined preparation and acquisition. m and T_1 values were obtained by fitting the data with Eq. (5)						
t_3 = 35 ms; t_2 = 30 ms	T_2 too short	T_2 too short	6.363	230	–	6.27

overestimate of the zero-time magnetisations in the CPMG acquisition sequence by the UPEN deconvolution programme and/or accumulating imperfections in the 180° pulses. The results also show that better agreement is obtained with the long T_1 component with longer echo spacings. The results for the periodically repeated t_2–t_3 spacing with separate preparation and accumulation have been included in Table 1 but it is clear from Fig. 4 that this sequence is not well suited to T_1 measurements because of its insensitivity to small differences in T_1 and this is confirmed by the near equality of the steady-state magnetisations for the two relaxation components. The results for the periodically repeated t_3–t_3–t_2 pulse spacing unit with separate preparation and acquisition are also shown in Table 1 and are comparable to those obtained with a single pulse spacing, t_e, although the t_3–t_3–t_2 has the added advantage that different components can be nulled by judicious choice of the pulse spacings.

Table 2 refers to the periodic sequences where the acquisition and preparation are combined into a single repeating unit. The results for a single echo spacing, t_e, show that the echo time t_e needs to be several tens of milliseconds to get measureable steady-state magnetisation which means that short T_2 components cannot be observed. The same is true for the combined t_3–t_3–t_2 sequence in Table 2 which implies that, in general, the periodic sequences with separate preparation and acquisition are more generally applicable than the combined periodic sequences. Because the constant echo spacing, t_e, sequence with separate preparation and acquisition appears to be the most flexible it was tested with a more realistic sample comprising sunflower oil. A conventional, slow, two-dimensional continuous inversion-recovery T_1–T_2-spectrum shows that the oil is triple exponential, but the third short T_1 component is minor with only ca. 4% of the intensity. It therefore presents a more challenging test sample than the double-doped water. Table 3 summarises the results of several repeat experiments which establish that the typical experimental error is ca. 1.2% for the long component, but 17% for the short component, possibly because the method fails to resolve the third minor relaxation component.

Table 3
Experimental steady-state longitudinal magnetisations, m%, for the short T_2 component (T_{2a} = 10.3 ms; T_{1a} = 56.7 ms) and long component (T_{2b} = 186 ms; T_{1b} = 243 ms) in sunflower oil measured with the FLOP–T_1–T_2 sequence in Fig. 2 with a single pulse spacing and separate preparation and acquisition. The 90–180 spacing in the acquisition CPMG sequence was 250 s for the short T_2 component and 2 ms for the long T_2 component. *m* and T_1 values were obtained by fitting the data with Eq. (4).

Pulse spacing, t_e (ms)	m_a (%)	T_{1a} (ms)	m_b (%)	T_{1b}(ms)
25	16.8	74	4.9	254
50	41.0	57	9.95	250
75	45.9	76	14.7	253
100	62.3	68.5	19.3	255.5
Mean T_1's		**69 ± 12**		**253 ± 3**

5. Discussion

In this paper we have explored various ways in which steady-state longitudinal magnetisation can be used to acquire two-dimensional T_1–T_2 spectra in a fast single-shot protocol. It is particularly interesting to note how the CPMG sequence establishes a steady-state in the longitudinal magnetisation which can be used not just for T_2 measurements but also for T_1 measurements. Our analysis shows that there are advantages and disadvantages to each of the sequences presented here. The simplest periodic sequence with a constant echo time, t_e, and with separate preparation and acquisition (Fig. 1 and the first sub-table in Table 1) is the best for fast determination of a T_1–T_2-spectrum such as that in Fig. 3. However, in its present form, it generates a "discrete" T_1–T_2-spectrum in the sense that the spectrum necessarily comprises a set of discrete spectral peaks as in Fig. 3 and not, for example, continuous distributions such as that in Fig. 9. Combining the preparation and acquisition in the way presented in Section 2.2, reduces the acquisition time but means that the same long echo spacings need to be used in the acquisition as in the preparation and because measureable steady-state magnetisation usually requires long echo spacings of tens of milliseconds, it means that

short T_2 components will be poorly characterised. The a-periodic sequence has the advantage that it gives a continuous T_1–T_2-spectrum such as that in Fig. 9, but suffers from the need for complete pre-calculation of all the pulse spacings using an average T_1 for the sample. The resulting T_1–T_2-spectrum is therefore distorted in the T_1 dimension because the pulse spacings are correct for the average T_1 but not for each component T_1.

The periodic FLOP–T_1–T_2 steady-state methodology can be extended in several ways. Diffusion can be measured by incorporating gradients into the periodic sequences. Perhaps the simplest example would be the case of separate preparation and acquisition where the acquisition CPMG sequences have an echo spacing 2τ and the preparation sequence a longer pulse spacing, t_e. Repeating this sequence in a constant gradient, G, introduces the diffusive attenuation factor, $\exp(-q^2Dt/3)$, where the wave vector q is $\gamma G\tau$. A discrete D–T_1–T_2 characterisation of the sample can therefore be done in a single shot because the establishment of steady-state longitudinal magnetisation does not depend on the applied gradient. It is also worth noting that full chemical shift information is retained in the spin-echoes, so that, in principle, Fourier transformation of the echoes acquired on a high field, high resolution spectrometer with and without the applied constant gradient should allow complete D–T_1–T_2 characterisation of each chemically shifted spectral peak in the sample.

Acknowledgments

The authors wish to thank their colleague, Ben Piggott for his encouragement and support. Brian Hills gratefully acknowledges funding support from the Biology and Biotechnology Science Research Council (BBSRC).

Appendix A

A.1. Derivation of the steady-state magnetisation for the [–t3a–t3a–t2–t3b–t3b–t2–] sequence

The time-evolution of the longitudinal magnetisation within the repeating unit in Fig. 6 is straightforward to calculate using a repeated application of the well-known solution to the Bloch equations for inversion recovery,

$$M(t) = M_\infty + [M(0) - M_\infty]\exp(-R_1 t) \tag{27}$$

where R_1 is the longitudinal relaxation rate, $1/T_1$, and M_∞ is the equilibrium longitudinal magnetisation. At the end of the t_{3a} period we have

$$M(t_{3a}) = M_\infty + (M_s - M_\infty)\exp(-R_1 t_{3a}) \tag{28}$$

This increase is reversed by flipping the magnetisation with a 180° pulse so that the magnitude now decreases, such that, after another t_{3ba} period we have,

$$M(2t_{3a}) = M_\infty + [-2M_\infty - (M_s - M_\infty)\exp(-R_1 t_{3a})] \times \exp(-R_1 t_{3a}) \tag{29}$$

A third 180° pulse now inverts the magnetisation and after an additional time delay, t_2 we have

$$M(t_2 + 2t_{3b}) = M_\infty + -2M_\infty - [-2M_\infty - (M_s - M_\infty) \times \exp(-R_1 t_{3a})]\exp(-R_1 t_{3a})\exp(-R_1 t_2) \tag{30}$$

Continuing in this way through the whole repeating pulse sequence unit it can be shown that the magnetisation at the end of the second t_2 period and before the inversion pulse is

$$m = (1 + B)/(1 - A) \tag{31}$$

where we have defined the normalised steady-state magnetisation, m, as the ratio M_s/M_∞ and M_s is the steady-state magnetisation indicated in figure X. The terms A and B are

$$A = \exp[-R_1 2(t_{3a} + t_{3b} + t_2)] \tag{32}$$

$$B = [-2 - [-2 - [-2 - [-2 - [-2 + \exp(-R_1 t_{3a})] \times \exp(-R_1 t_{3a})]\exp(-R_1 t_2)]\exp(-R_1 t_{3b})]\exp(-R_1 t_{3b})] \times \exp(-R_1 t_2) \tag{33}$$

and it can be seen that the B term reflects the structure of the repeating pulse sequence unit. The relationship between the pulse spacings at the null point, $m = 0$, is obtained by solving the equation $B = -1$. These equations are straightforward to solve numerically with a MATLAB programme and the 2D plot in Fig. 2 shows representative results for the absolute value of the total steady-state magnetisation, $m(t_{3a},t_{3b})$ for a fixed value of t_2 and for a model three-component sample having T_1 values of 10, 50 and 100 ms in equal proportions.

References

[1] Y.-Q. Song et al., T_1–T_2 correlation spectra obtained using a fast 2D Laplace Inversion, J. Magn. Reson. 154 (2002) 261–268.
[2] M.D. Hurlimann, L. Venkataramanan, Quantitative measurements of 2D distribution functions of diffusion and relaxation in grossly inhomogeneous fields, J. Magn. Reson. 157 (2002) 31–42.
[3] P.J. McDonald, J.-P. Korb, J. Mitchell, L. Monteilhet, Surface relaxation and chemical exchange in hydrating cement pastes: two-dimensional NMR relaxation study, Phys. Rev. E72 E72 (011409) (2005) 1–9.
[4] B.P. Hills, Relaxometry: two-dimensional methods, in: R. Harris, R. Wasylishen (Eds.), Electronic Encyclopedia of Magnetic Resonance, 2009. <http://mrw.interscience.wiley.com/emrw/9780470034590/home/>.
[5] N. Marigheto, L. Venturi, B.P. Hills, Two-dimensional NMR relaxation studies of apple quality, Postharvest Biol. Technol. 48 (2008) 331–340.
[6] L. Venturi, N. Woodward, D. Hibberd, N. Marigheto, A. Gravelle, G. Ferrante, B.P. Hills, Multidimensional cross-correlation relaxometry of aqueous protein systems, Appl. Magn. Reson. 33 (2008) 213–234.
[7] D. Austin, B.P. Hills, Two-dimensional NMR relaxation studies of the pore structure in silicone hydrogel contact lenses, Appl. Magn. Reson. 35 (2009) 581–591.
[8] J. Warner, S. Donnell, K.M. Wright, L. Venturi, B.P. Hills, The characterisation of mammalian tissue with 2D relaxation methods, Magn. Reson. Imaging, in press.
[9] G. Saab, R.T. Thompson, G.D. Marsh, P.A. Picot, G.R. Moran, Two-dimensional time correlation relaxometry of skeletal muscle *in vivo* at 3 Tesla, Magn. Reson. Med. 46 (2001) 093–1098.
[10] L. Venturi, J. Warner, B.P. Hills, Multisliced ultrafast 2D relaxometry, Magn. Reson. Imaging, in press.
[11] L. Venturi, B.P. Hills, Spatially-resolved multidimensional cross-correlation relaxometry, Magn. Reson. Imaging 28 (2010) 71–177.
[12] L. Venturi, B.P. Hills, Fast T_1 mapping by flipped longitudinal polarisation (FLOP), Magn. Reson. Imaging., in press.
[13] D.M. Doddrell, W.M. Brooks, J.M. Bulsing, J. Field, M.G. Irving, H. Baddeley, Spatial & chemical shift encoded excitation. SPACE, A new technique for volume-selected NMR spectroscopy, J. Magn. Reson. 68 (1986) 367–372.
[14] G.C. Borgia, R.J.S. Brown, P. Fantazzini, Uniform penalty inversion of multiexponential decay data, J. Magn. Reson. 132 (1998) 65–77.
[15] G.C. Borgia, R.J.S. Brown, P. Fantazzini, Uniform penalty inversion of multiexponential decay data II, data spacing, T_2 data, systematic data errors and diagnostics, J. Magn. Reson. 147 (2000) 273–285.
[16] J. Frahm, A. Haase, D. Matthaei, Rapid NMR imaging of dynamic processes using the FLASH technique, Magn. Reson. Med. 3 (1986) 321–327.